

Encounters between Dynamic Cortical Microtubules Promote Ordering of the Cortical Array through Angle-Dependent Modifications of Microtubule Behavior ^W

Ram Dixit¹ and Richard Cyr

Penn State University, University Park, Pennsylvania 16802

Ordered cortical microtubule arrays are essential for normal plant morphogenesis, but how these arrays form is unclear. The dynamics of individual cortical microtubules are stochastic and cannot fully account for the observed order; however, using tobacco (*Nicotiana tabacum*) cells expressing either the MBD-DsRed (microtubule binding domain of the mammalian MAP4 fused to the *Discosoma* sp red fluorescent protein) or YFP-TUA6 (yellow fluorescent protein fused to the Arabidopsis α -tubulin 6 isoform) microtubule markers, we identified intermicrotubule interactions that modify their stochastic behaviors. The intermicrotubule interactions occur when the growing plus-ends of cortical microtubules encounter previously existing cortical microtubules. Importantly, the outcome of such encounters depends on the angle at which they occur: steep-angle collisions are characterized by approximately sevenfold shorter microtubule contact times compared with shallow-angle encounters, and steep-angle collisions are twice as likely to result in microtubule depolymerization. Hence, steep-angle collisions promote microtubule destabilization, whereas shallow-angle encounters promote both microtubule stabilization and coalignment. Monte Carlo modeling of the behavior of simulated microtubules, according to the observed behavior of transverse and longitudinally oriented cortical microtubules in cells, reveals that these simple rules for intermicrotubule interactions are necessary and sufficient to facilitate the self-organization of dynamic microtubules into a parallel configuration.

INTRODUCTION

The vast majority of plant cells contain an ordered cortical microtubule array that is important for plant morphogenesis because it affects the ordered deposition of cellulose microfibrils in most anisotropically growing cells (Cyr, 1994; Baskin, 2001; Wasteneys, 2002). The ability of the cell to deposit cellulose microfibrils in an ordered configuration is typically dependent upon the cortical microtubules: a disorganized cortical microtubule array is usually associated with disorganized nascent cellulose microfibrils and isotropic cell growth (Williamson, 1991; Baskin, 2001; Burk and Ye, 2002; Sugimoto et al., 2003; Baskin et al., 2004). Hence, to understand how cells undergo anisotropic growth, more insight is needed into how cortical microtubules achieve and maintain parallel organization in elongating cells.

The cortical microtubules in a rapidly elongating cell are predominantly oriented transverse to the elongation axis (Lloyd, 1994; Sugimoto et al., 2000; Granger and Cyr, 2001). Importantly,

this array pattern is not a result of microtubule nucleation in the appropriate configuration, but rather a result of the progressive organization of cortical microtubules after nucleation (Wasteneys and Williamson, 1989; Hepler et al., 1993; Wasteneys et al., 1993; Yuan et al., 1994; Wymer et al., 1996). The sequence of cortical microtubule organization—from a random arrangement, to regional organization, and ultimately global organization—is observed during both normal and experimental conditions, suggesting that there is a single, conserved mechanistic route for cortical microtubule organization (Cyr, 1994). However, the details regarding this mechanism are not well understood.

As with other eukaryotes, plant microtubules are primarily composed of α - and β -tubulins, which have the ability to self-assemble into 25-nm microtubules (Goddard et al., 1994). The direct observation of individual cortical microtubules in living cells has revealed that these microtubules are highly dynamic and display periods of growth (polymer assembly) and shrinkage (polymer disassembly), interspersed by stochastic transitions between these two phases, as described by the dynamic instability model (Chan et al., 2003; Dhonukshe and Gadella, 2003; Mathur et al., 2003; Shaw et al., 2003; Vos et al., 2004). In addition, cortical microtubules show a treadmilling-type behavior with the leading end (plus-end) undergoing polymerization-biased dynamics and the lagging end (minus-end) undergoing slow depolymerization. This type of microtubule assembly dynamics results in apparent polymer displacement over time (Shaw et al., 2003; Vos et al., 2004). Microtubule assembly dynamics can regulate their spatial and temporal organization; however, the stochastic dynamics of individual cortical

¹To whom correspondence should be addressed. E-mail rvd10@psu.edu; fax 814-865-9131.

The authors responsible for distribution of materials integral to the findings presented in this article in accordance with the policy described in the Instructions for Authors (www.plantcell.org) are: Ram Dixit (rvd10@psu.edu) and Richard Cyr (rjc8@psu.edu).

^WOnline version contains Web-only data.

Article, publication date, and citation information can be found at www.plantcell.org/cgi/doi/10.1105/tpc.104.026930.

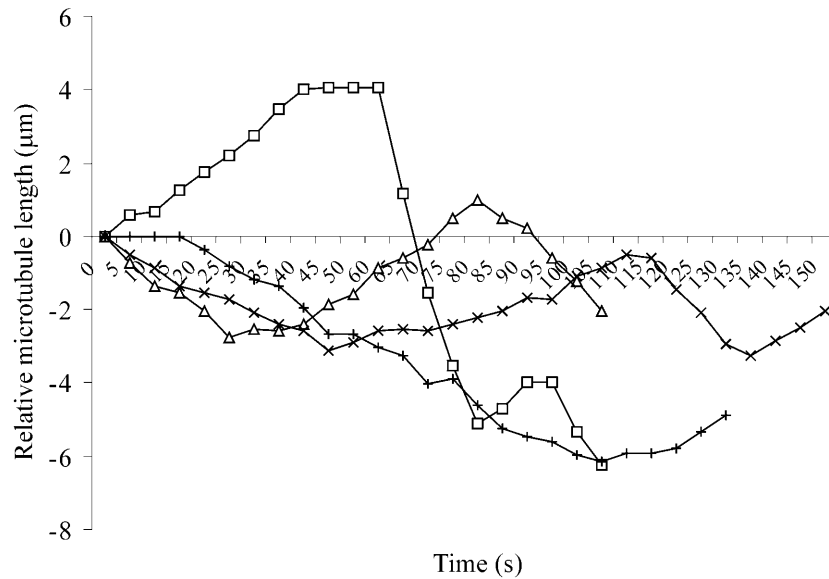


Figure 1. Life History Plots of Individual Cortical Microtubule Plus-Ends.

Microtubule dynamics were visualized in MBD-DsRed-expressing cells by time-lapse microscopy using 1-s exposures to capture images at 5-s intervals for several minutes. The change in length, relative to the starting position, of individual microtubule plus-ends was determined frame-by-frame and used for the life history plots. The life history plots of four separate cortical microtubules are shown. Dynamic instability parameters were determined for each microtubule using the life history plots and the criteria described in Methods.

microtubules alone are unlikely to account for their ordered arrangement into a parallel configuration.

Although the primary constituent of microtubules is tubulin, a variety of other proteins, termed microtubule-associated proteins (MAPs), interact with microtubules and regulate their assembly properties, their associations with other cellular structures, and their ability to participate in various intracellular transport activities (Azimzadeh et al., 2001; Reddy, 2001; Hussey et al., 2002; Gardiner and Marc, 2003; Hashimoto, 2003; Wasteney and Galway, 2003). Of special importance to the cortical array are those MAPs that facilitate the attachment of microtubules to the plasma membrane (Lloyd et al., 1996). One of these MAPs is phospholipase D (Gardiner et al., 2001), and activators of this important signaling moiety induce the detachment of microtubules from the plasma membrane (Dhonukshe et al., 2003), along with a concomitant disordering of the detached microtubules and a loss of growth anisotropy (Dhonukshe et al., 2003; Gardiner et al., 2003). Hence, plasma membrane attachment is critical for cortical microtubule organization and function. An important feature of plasma membrane attachment is that cortical microtubules are effectively confined to a thin shell that can be modeled as a two-dimensional surface.

Microtubule assembly dynamics govern how much polymer exists in the cortical array, but how this behavior leads to the highly organized arrays warrants consideration. In other words, how does a large population of dynamic cortical microtubules become organized into ordered arrays along the entire length of the cell? Cortical microtubules exist in a complex nonequilibrium state, and the cortical microtubule array patterns are not static but rather continuously dynamic. For example, observations on

living cells show that the transverse alignment of cortical microtubules is not absolute and static, but can shift within certain spatial limits (Marc et al., 1998). This property raises the possibility that collective, local interactions among individual cortical microtubules (with all of their associated proteins) leads to the emergence of a globally ordered cortical array that is continuously dynamic. The rules that govern the local organization of microtubules likely act in a non-scalable fashion (i.e., fractal) because self-organization of the cortical array appears to follow fractal rules (Wasteney, 2002).

Table 1. Dynamic Instability Properties of Cortical Microtubules during Interphase

Dynamic Instability Parameters	MBD-DsRed	YFP-TUA6
Growth rate ($\mu\text{m}/\text{min}$)	5.60 ± 1.92 (64)	6.15 ± 3.05 (23)
Shrinkage rate ($\mu\text{m}/\text{min}$)	10.09 ± 3.52 (92)	10.03 ± 3.11 (35)
f_{rescue} (events/min)	3.26 ± 1.75 (61)	2.99 ± 1.83 (12)
$f_{\text{catastrophe}}$ (events/min)	1.61 ± 1.40 (56)	2.32 ± 1.51 (22)
Dynamicity ($\mu\text{m}/\text{min}$)	6.91 ± 3.28 (114)	6.98 ± 3.04 (51)
Growth time	31%	33%
Shrinkage time	40%	42%
Pause time	29%	25%

The data represent the average \pm SD (n = microtubules) for the plus-ends of microtubules in either MBD-DsRed- or YFP-TUA6-expressing BY-2 cells. The dynamic instability parameters are statistically indistinguishable between the two cell lines (P -value $>$ 0.05 using the t test). f_{rescue} , frequency of microtubule rescue events; $f_{\text{catastrophe}}$, frequency of microtubule catastrophe events.

Here, we present quantitative data that describe the non-random modification of cortical microtubule dynamics as a result of intermicrotubule encounters. The data show that the dynamic behavior of cortical microtubules is modified depending on the angle at which they encounter each other. We propose that this behavior exemplifies two fundamental rules of self-organization in this array: namely, zippering of microtubules after shallow-angle encounters to promote their coalignment and bundling and catastrophic collisions after steep-angle encounters to promote the biased-turnover of nonparallel microtubules. In other words, the microtubule dynamics are modified by their relative orientation such that microtubules grow longer and persist for a greater length of time when they are arranged in a parallel manner. Using a Monte Carlo modeling technique, we verified this prediction and show that local self-organization of microtubules can be simulated by modifying the stochastic parameters of microtubules as a function of their interactions in a two-dimensional plane. The results are consistent with the hypothesis that intermicrotubule interactions are necessary and sufficient for the parallel organization of cortical microtubules.

RESULTS

Observation of Individual Cortical Microtubule Dynamics during Interphase

Time-lapse fluorescence microscopy was used to visualize individual cortical microtubule dynamics in tobacco (*Nicotiana tabacum*) Bright Yellow-2 (BY-2) cells expressing either the MBD-DsRed (microtubule binding domain of the mammalian

MAP4 fused to the *Discosoma* sp red fluorescent protein; Dixit and Cyr, 2003) or YFP-TUA6 microtubule markers (yellow fluorescent protein fused to the Arabidopsis α -tubulin 6 isoform; Ueda et al., 1999). Cells with a predominantly transverse cortical microtubule array were used for observations. Microtubule dynamic instability parameters were determined from life history plots of individual microtubules during interphase (Figure 1; see Supplemental Movie 1 online). The dynamics of the cortical microtubules were statistically indistinguishable in both cell lines (Table 1), and they are in reasonable agreement with previously reported values for plant cortical microtubules (Chan et al., 2003; Dhonukshe and Gadella, 2003; Mathur et al., 2003; Shaw et al., 2003; Vos et al., 2004). The MBD-DsRed cell line was preferred in this study because this marker required less-damaging excitation wavelengths (Dixit and Cyr, 2003) and because of the higher signal-to-noise ratio of the microtubule images. However, it is important to note that similar results were obtained using both cell lines.

Encounters between Cortical Microtubules Affect Their Dynamic Behavior

Most cortical microtubules in these cell lines, as with cells expressing other microtubule markers (Granger and Cyr, 2001; Chan et al., 2003; Dhonukshe and Gadella, 2003; Dhonukshe et al., 2003; Shaw et al., 2003; Vos et al., 2004), remain in focus for extended periods of time and therefore appear to be plasma membrane attached. The criterion of focal plane stability is a reliable indicator of cortical microtubule attachment to the plasma membrane because the loss of plasma membrane

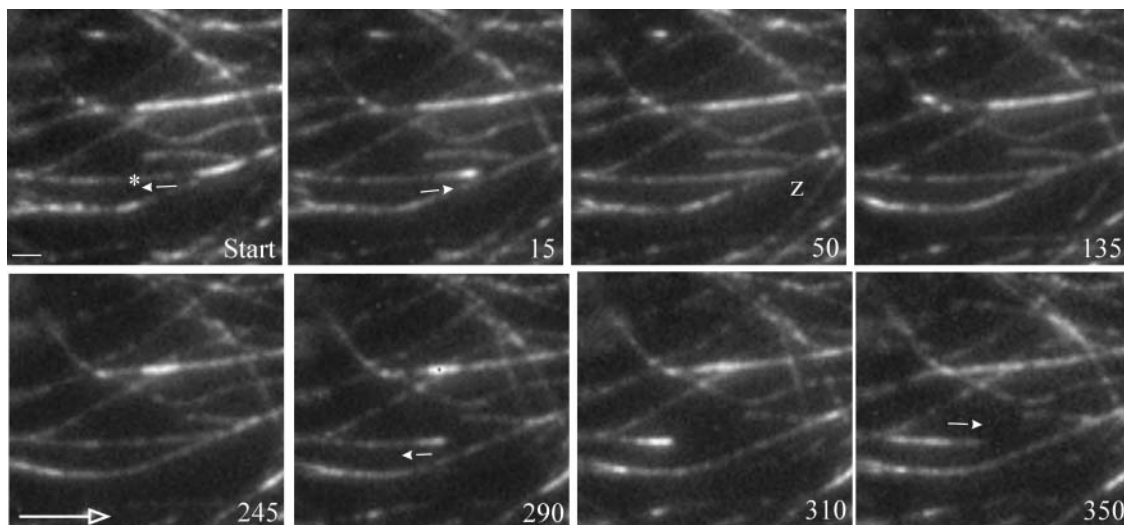


Figure 2. Zippering of Microtubules after Shallow-Angle Encounters.

The outcome of shallow-angle encounters between cortical microtubules in MBD-DsRed-expressing cells is shown. The microtubule of interest is marked by an asterisk, and the small arrows denote the onset of microtubule polymerization or depolymerization. The large open arrow shows the transverse direction with respect to the cell elongation axis. The numbers denote time in seconds. A microtubule undergoes a catastrophe event followed quickly by a rescue event, which leads to a shallow-angle (20°) encounter with a preexisting microtubule at 50 s (z). These two microtubules remain in contact for a relatively long time (~ 240 s) before a second catastrophe event (at 290 s) results in depolymerization of the zippered microtubule. However, the microtubule does not completely depolymerize and eventually starts growing again after a second rescue event. Scale bar = $2 \mu\text{m}$.

attachment leads to a rapid and sustained blurring of the microtubule image because of the streaming movement of the detached microtubule (also see Dhonukshe et al., 2003; Shaw et al., 2003; Vos et al., 2004). The plasma membrane attachment of cortical microtubules is important because it effectively restricts their behavior within a two-dimensional plane.

In a two-dimensional plane, growing cortical microtubule ends can encounter preexisting cortical microtubules that are also plasma membrane attached. Observations of cortical microtubules in MBD-DsRed expressing cells revealed that such intermicrotubule encounters are frequent and that they are associated with either of three types of outcomes: (1) the encountering microtubule changes its trajectory and becomes increasingly laterally associated and coaligned with the preexisting microtubule (termed microtubule zippering; Figure 2); (2) the encountering microtubule stops growing and rapidly transitions to catastrophe (termed catastrophic collision; Figures 3A

and 3B); or (3) the encountering microtubule appears unaffected by the encounter and continues growing in its original trajectory (termed crossover; Figure 3B). Similar observations were obtained using YFP-TUA6 expressing cells (see Supplemental Figure 1 online).

Interestingly, analysis of the distribution of the encounter angles associated with each of these outcomes shows that the outcome of an intermicrotubule encounter is strongly influenced by the angle at which the encounter occurred in both MBD-DsRed and YFP-TUA6 expressing cells (Figure 4). Specifically, shallow-angle encounters ($<40^\circ$) are associated with microtubule zippering, whereas steep-angle encounters ($>40^\circ$) are associated with catastrophic collisions or microtubule crossover. Approximately 90% of the shallow-angle encounters led to microtubule zippering at an average contact angle of $24 \pm 10^\circ$ ($n = 87$ microtubules). Only $\sim 15\%$ of the shallow-angle encounters led to microtubule catastrophe (average contact angle of

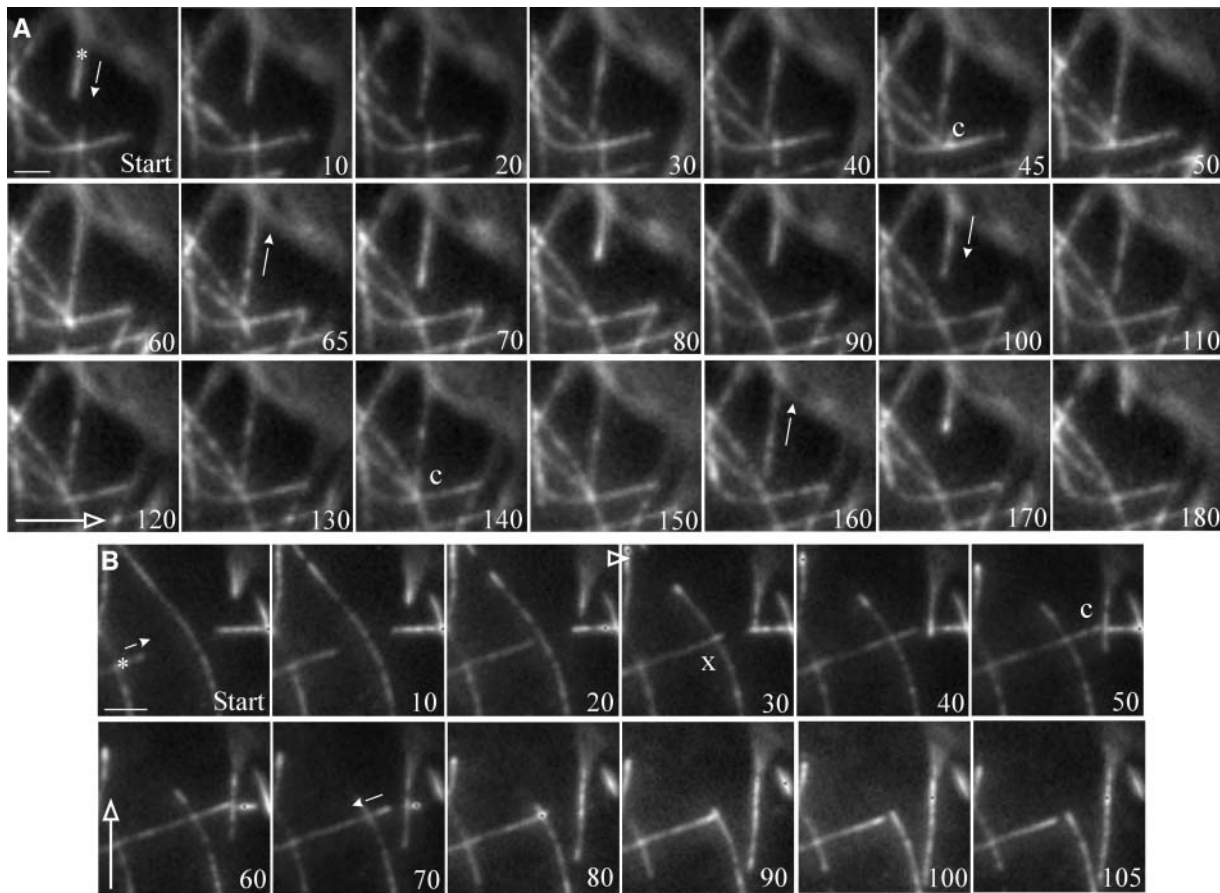


Figure 3. Catastrophic Collisions between Cortical Microtubules after Steep-Angle Encounters.

The outcome of steep-angle encounters between cortical microtubules in MBD-DsRed-expressing cells is shown. The microtubule of interest is marked by an asterisk, and the small arrows denote the onset of microtubule polymerization or depolymerization. The large open arrows show the transverse direction with respect to the cell elongation axis. The numbers denote time in seconds.

(A) A growing cortical microtubule has a steep-angle (73°) encounter at 45 s (c) with a preexisting microtubule and depolymerizes after ~ 20 s of contact. The microtubule then undergoes a rescue event and has a second steep-angle (73°) encounter (at 140 s), followed rapidly by depolymerization.

(B) A growing cortical microtubule has a steep-angle (75°) encounter with a preexisting microtubule, which it crosses over (x), and continues growing. This microtubule then has a second steep-angle (70°) encounter at 50 s (c), which is followed rapidly by a catastrophe. Scale bars = $2 \mu\text{m}$.

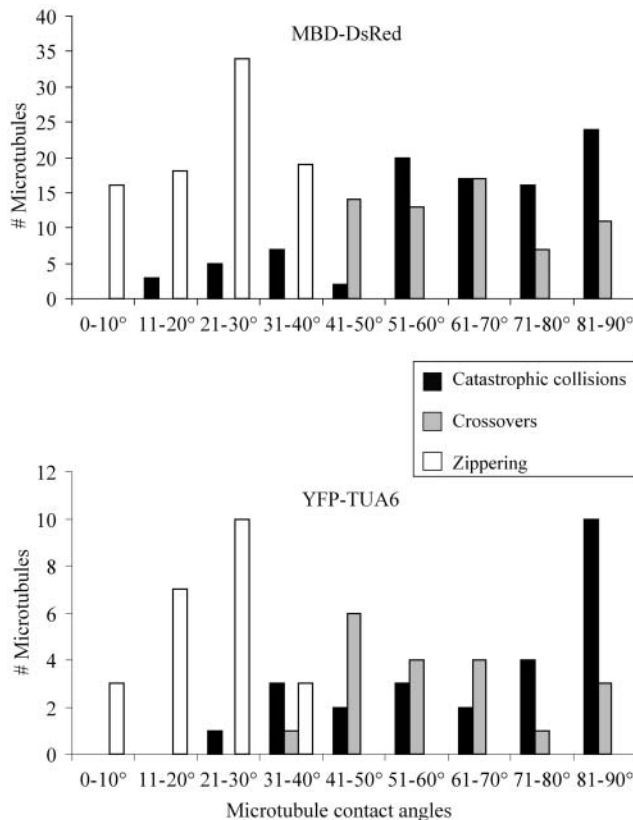


Figure 4. Relationship between Microtubule Contact Angles and the Outcome of Intermicrotubule Encounters.

The histograms show the distribution of the contact angles associated with catastrophic collisions (black bars), microtubule crossovers (gray bars), and microtubule zippering (white bars) in MBD-DsRed- and YFP-TUA6-expressing cells. Note the correlation between microtubule zippering and shallow contact angles and between catastrophic collisions and steep contact angles. The observed cutoff angle between these responses is $\sim 40^\circ$.

$28 \pm 8^\circ$; $n = 15$ microtubules). By contrast, $\sim 60\%$ of the steep-angle encounters led to microtubule catastrophe at an average contact angle of $72 \pm 14^\circ$ ($n = 82$ microtubules). This angle is significantly greater than the average contact angle of $65 \pm 14^\circ$ ($n = 62$ microtubules) associated with microtubule crossover (P-value ~ 0.01), which indicates that the probability for microtubule catastrophe is higher with increasingly steep contact angles.

Note that microtubule zippering and catastrophic collisions apparently were not dependent on whether the microtubule plus-ends were oriented parallel or antiparallel to each other (as determined by the orientations of the visible growing ends during some encounters), but rather on the absolute contact angle.

Catastrophic Collisions and Zippering of Microtubules as Antagonistic Modifiers of Cortical Microtubule Dynamics

Modification of the stochastic nature of microtubule assembly dynamics through microtubule encounters could result in a

nonrandom organization of the cortical microtubule array. Quantification of the microtubule contact time in MBD-DsRed and YFP-TUA6 expressing cells, after encounters, shows that the average contact time after microtubule zippering is approximately sevenfold greater than the average contact time after catastrophic collisions (Table 2; see Supplemental Table 1 online). In other words, catastrophic collisions rapidly lead to microtubule depolymerization, whereas microtubule zippering results in microtubule association for relatively long periods of time.

Interestingly, the microtubule contact time for zippering longitudinal microtubules is significantly shorter than the contact time for zippering transverse microtubules (Table 2; see Supplemental Table 1 online). In addition, longitudinal microtubules have a higher probability for catastrophic collisions ($\sim 60\%$) as compared with transverse microtubules ($\sim 20\%$). This difference is related to the fact that the bulk of the microtubules in an elongating BY-2 cell are oriented transverse to the elongation axis. As a result, there is a greater tendency for microtubule zippering to occur between transverse microtubules as compared with longitudinal microtubules.

Quantification of the frequency of microtubule depolymerization, after microtubule encounters, revealed that catastrophic collisions are twice as likely to lead to microtubule depolymerization as compared with microtubule zippering. Taken together, the data suggest that catastrophic collisions promote microtubule destabilization, whereas microtubule zippering promotes microtubule stabilization and coalignment.

Monte Carlo Simulations Reveal Self-Organization of Microtubules through Intermicrotubule Encounters

The modification of microtubule dynamics by intermicrotubule encounters can potentially result in the self-organization of cortical microtubules into a parallel configuration. A Monte Carlo modeling technique was implemented to determine whether these rules can simulate local ordering of microtubules from a randomly oriented population of simulated microtubules.

Table 2. Microtubule Contact Times after Zippering and Catastrophic Collisions in MBD-DsRed-Expressing Cells

Microtubule Orientation Relative to the Cell Axis	Contact Time (s)	
	Zippering	Catastrophic Collision
Transverse	157 ± 89 (41)	23 ± 14 (13) ^a
Longitudinal	83 ± 25 (12) ^b	20 ± 10 (20) ^c

The data represent the average microtubule contact times \pm SD ($n =$ microtubules) after microtubule zippering or catastrophic collisions.

^a Comparison between the contact times for zippering and catastrophically colliding transverse microtubules: P-value ~ 0.0001 (Mann-Whitney test).

^b Comparison between the contact times for zippering transverse and longitudinal microtubules: P-value ~ 0.004 (Mann-Whitney test).

^c Comparison between the contact times for zippering and catastrophically colliding longitudinal microtubules: P-value ~ 0.001 (Mann-Whitney test).

A randomly oriented population of 20 simulated microtubules was subjected to iterative Monte Carlo modeling of microtubule behavior based on the criteria shown in Tables 1 and 2 (see Methods for further details). The model reveals that successive iterations result in a constriction of the distribution of angles within the microtubule population (Figure 5; see Supplemental Movie 2 online). Discordant microtubules, having a tendency toward catastrophic collisions, tend to be lost, whereas microtubules that demonstrate zippering tend to be maintained and become bundled. Eventually, there is an emergence of a local organization of microtubules into a parallel configuration (Figure 5, right panel). A similar outcome was obtained for four independent repeats of this modeling technique (starting with new microtubule positions). It is important to note that the final predominant microtubule angle was different in each of the independent simulations. Hence, additional work is needed to understand the rules governing the establishment of a transverse array.

Test simulations that assigned the same contact time constraint (of 1 min) for zippering transverse versus longitudinal microtubules also resulted in local self-organization of microtubules in two separate trials (see Supplemental Figure 2 online).

In other words, the self-organization of microtubules, at least under the conditions employed in these simulations, did not depend on differences in contact time properties between transverse and longitudinal zippering microtubules.

Control Monte Carlo simulations, starting with the same initial microtubule positions as the experimental runs but without imposing the constraints of catastrophic collisions and microtubule zippering, did not result in the ordering of the simulated microtubules in three separate simulations (Figure 6; see Supplemental Movie 3 online). In these control simulations, the microtubules did not form bundles and did not show the emergence of a predominant microtubule angle. Furthermore, control simulations starting with short microtubules also did not result in the emergence of microtubule bundling and a predominant microtubule angle (Figure 7; see Supplemental Movie 4 online). In this case, the short microtubules never encountered each other; therefore, their dynamic behavior was not subject to regulation by microtubule interactions. Additional control simulations that used either only the zippering constraint or only the catastrophic collision constraint also did not result in significant microtubule self-organization (see Supplemental Figures 3 and 4

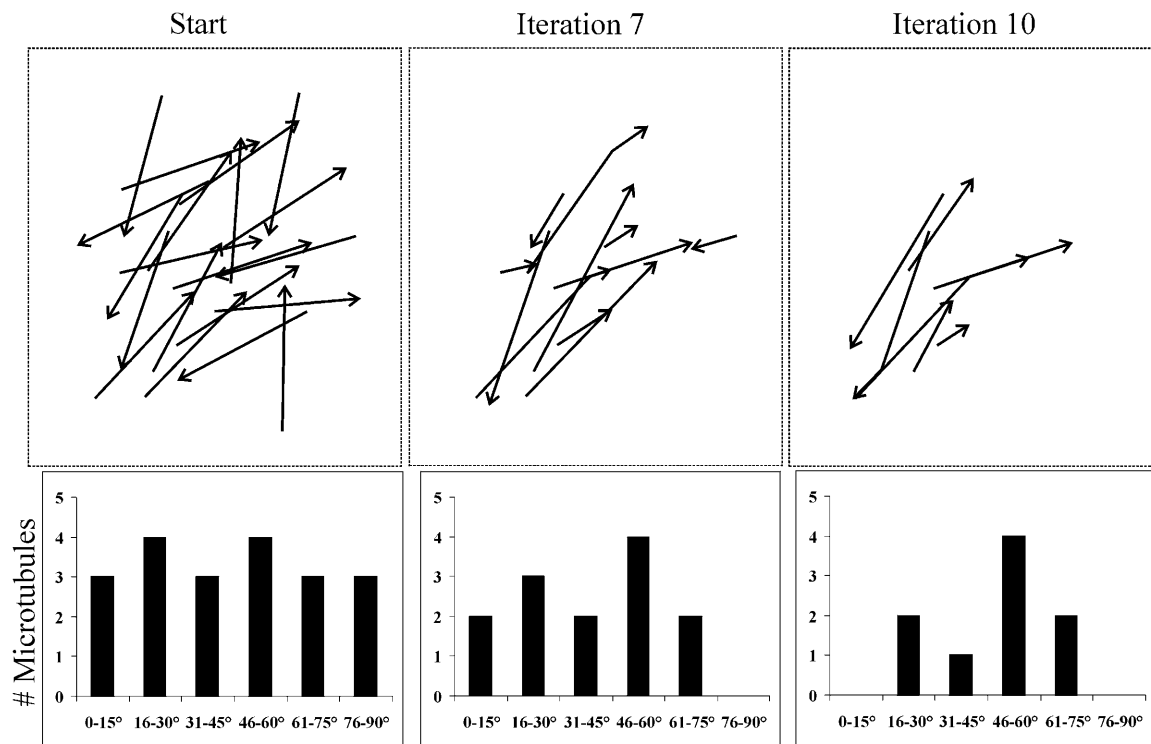


Figure 5. Emergence of Local Order from a Randomly Oriented, Simulated Microtubule Population.

The dynamic behavior of interphase cortical microtubules was simulated starting with a randomly oriented population of 20 simulated microtubules. These “microtubules” were subjected to an iterative Monte Carlo modeling technique, based on the parameters defining the stochastic dynamics of individual cortical microtubules, and the rules of modification of these parameters, based on microtubule encounter angles. Each iteration represents a span of 1 min. The starting condition shows the initial distribution of the microtubule angles. By iteration 7, it is apparent that some microtubule orientations (e.g., 0 to 15° and 76 to 90°) are not favored and that these microtubules are selectively depolymerized. By contrast, other microtubule orientations (46 to 60°) are selectively stabilized and persist over time. As a result, the distribution of microtubule angles narrows over time. By iteration 10, a predominant microtubule orientation (46 to 60°) is clearly established, reflecting a local, parallel microtubule organization.

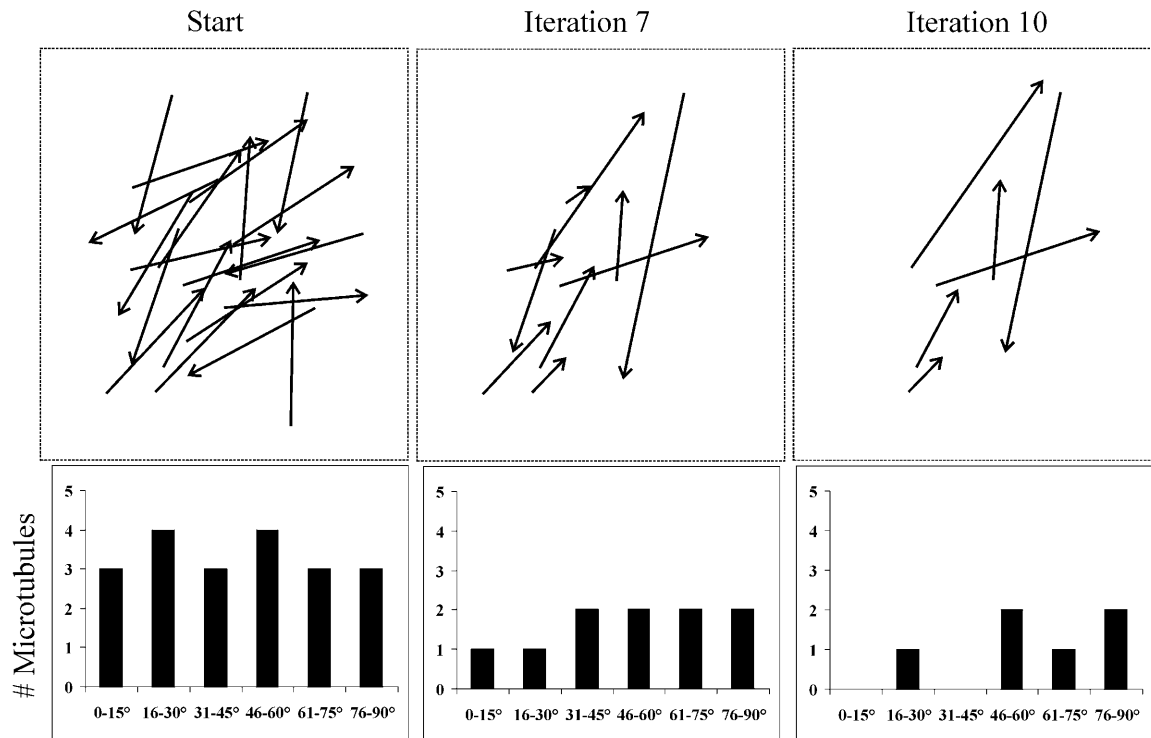


Figure 6. Lack of Microtubule Organization in the Absence of Microtubule Zippering and Catastrophic Collisions.

The dynamic behavior of interphase cortical microtubules was simulated starting with the same microtubule configuration as in Figure 5. These “microtubules” were subjected to an iterative Monte Carlo modeling technique, based solely on the parameters defining the stochastic dynamics of individual cortical microtubules. Each iteration represents a span of 1 min. The starting condition shows the initial distribution of the microtubule angles. By iteration 7, there is no hint of a predominant microtubule orientation, and by iteration 10, the microtubules remain randomly arranged.

online). These results indicate that the concerted action of both microtubule zippering and catastrophic collisions is required for the parallel organization of microtubules.

DISCUSSION

The plant cortical microtubules are typically organized into ordered arrays, and the function of the cortical microtubule cytoskeleton is intimately connected to the array pattern (for reviews, see Wasteneys, 2002; Hashimoto, 2003; Smith, 2003; Lloyd and Chan, 2004). During interphase, the cortical microtubule cytoskeleton consists of thousands of short, bundled microtubules that are dispersed throughout the cell cortex (Hardham and Gunning, 1978; Vesik et al., 1996). These microtubules are highly dynamic and are nucleated at random orientations throughout the cortex (Shaw et al., 2003). Therefore, a fundamental problem relating to the cortical microtubule cytoskeleton is how such a large population of dynamic elements becomes organized and maintains a parallel configuration.

The parallel configuration of the cortical microtubules is unlikely to result solely from the stochastic behavior of the individual microtubules. Computer simulations of microtubule array organization show that microtubule ordering requires the modification of the stochastic behavior of microtubules through the action

of external factors such as motor proteins (Vorobjev et al., 2001; Nedelec, 2002; Cytrynbaum et al., 2004), pigment granules (McNiven and Porter, 1988; Vorobjev et al., 2001), or geometric constraints (Maly and Borisy, 2002). In the case of higher plant cells, motor proteins are unlikely to be involved in the parallel organization of cortical microtubules because motor-driven cortical microtubule translocation has not been detected (Shaw et al., 2003; Vos et al., 2004). However, our observations show that intermicrotubule interactions modify the stochastic dynamics of cortical microtubules in a nonrandom fashion depending on the angle at which microtubule encounters occur. Specifically, shallow-angle (<40°) encounters promote microtubule coalignment and bundling (zippering), whereas steep-angle encounters promote microtubule depolymerization (catastrophic collisions). These intermicrotubule interactions therefore provide a mechanism for the establishment and maintenance of parallel cortical microtubule organization.

Microtubule zippering directly promotes microtubule parallelism by coaligning and bundling the interacting microtubules. Cortical microtubule bundling is significant because it is associated with increased microtubule stability and the formation of a higher order microtubule structure that spans the circumference of the cell (Hardham and Gunning, 1978; Cyr and Palevitz, 1989; Schellenbaum et al., 1992; Chan et al., 1999; Smertenko

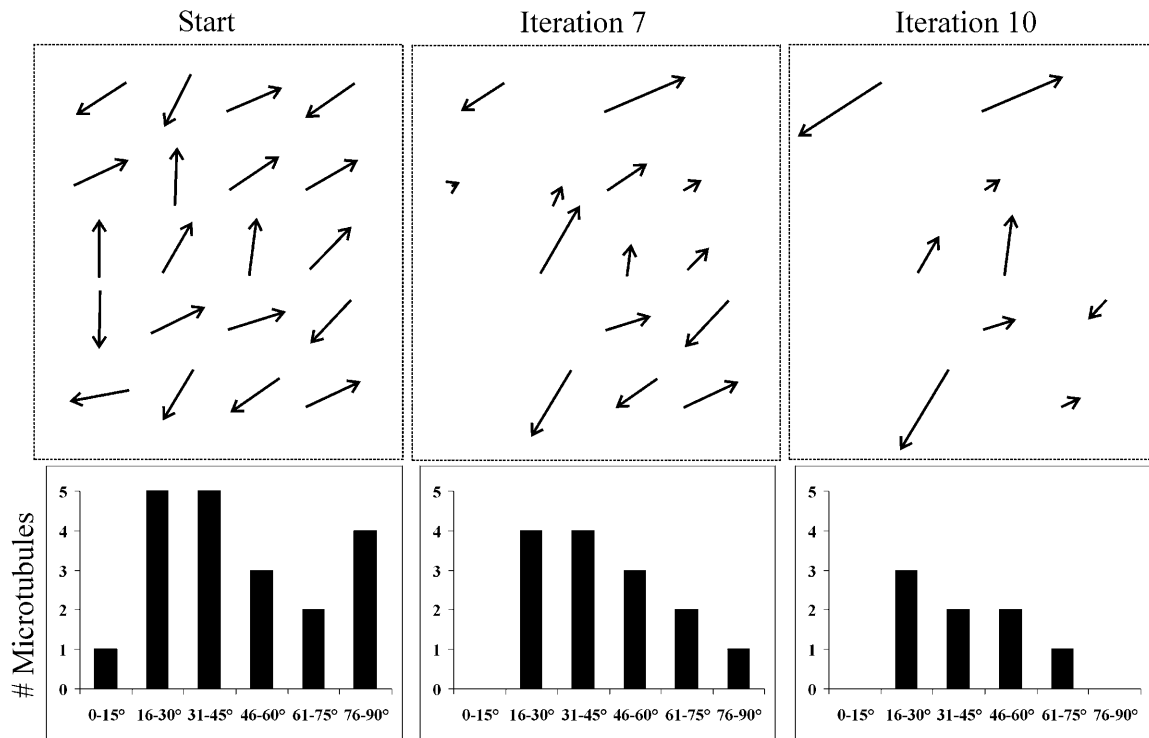


Figure 7. Lack of Microtubule Organization in the Absence of Intermicrotubule Interactions.

The dynamic behavior of interphase cortical microtubules was simulated starting with a randomly oriented population of 20 simulated microtubules. These “microtubules” were subjected to an iterative Monte Carlo modeling technique, based on the parameters defining the stochastic dynamics of individual cortical microtubules, and the rules of modification of these parameters, based on microtubule encounter angles. Each iteration represents a span of 1 min. The starting condition shows the initial distribution of the microtubule angles. Because these simulated microtubules are short, they do not undergo microtubule encounters; therefore, they do not display any microtubule bundling or microtubule reorientation by iteration 7. As a consequence of the lack of any microtubule interactions, the dynamics of these microtubules are purely stochastic, and the microtubules remain randomly arranged by iteration 10.

et al., 2000; Sonobe et al., 2001). The bundling activity may be attributable to cross-linking MAPs, such as certain MAP65 isoforms, which bundle and consequently stabilize adjacent microtubules (Jiang and Sonobe, 1993; Chan et al., 1999; Wicker-Planquart et al., 2004). Shallow-angle microtubule encounters could sterically facilitate the formation of MAP65 cross-bridges between the interacting microtubules and therefore result in microtubule zippering.

In rapidly elongating cells, microtubule zippering predominantly occurs between transverse microtubules because this is the predominant orientation of the cortical microtubules in these cells. This would predictably foster the stabilization and maintenance of transverse microtubule arrays in elongating plant cells. Furthermore, the relatively rare microtubule zippering events between nontransverse (longitudinal) microtubules, in these cells, are associated with significantly shorter contact times, as compared with the contact times for zippering transverse microtubules. This difference is not associated with significantly different dynamic instability parameters or mean zippering angle between transverse and longitudinal microtubules (data not shown). The shorter zippering contact time of longitudinal micro-

tubules may be attributable to the higher probability of these microtubules making a subsequent steep-angle encounter (and consequently depolymerizing) with the predominantly transverse microtubules. The low probability of zippering and stabilization of longitudinal microtubules also predictably contributes to the maintenance of the net transverse orientation of the cortical array in rapidly elongating cells.

Steep-angle ($>40^\circ$) microtubule collisions promote microtubule destabilization and the biased turnover of microtubules with discordant orientations. The selective loss of discordant microtubules (which arise as a result of the random cortical microtubule nucleation pattern) because of catastrophic collisions can also contribute to the formation and maintenance of a parallel microtubule organization. Specifically, the selective loss of discordant microtubule orientations through subsequent generations of cortical microtubules, thus promoting microtubule parallelism.

Steep-angle encounters may induce microtubule catastrophe because of the pushing forces generated by such encounters. Mechanical forces significantly decrease microtubule growth

velocity (Dogterom and Yurke, 1997), and in vitro experiments show that microtubules encountering a barrier undergo force-induced catastrophe (Janson et al., 2003). The observation that the probability of catastrophic collision is greater as the contact angle increases is consistent with the observation that increasing mechanical forces shorten the microtubule-barrier contact time (Janson et al., 2003). Predictably, the steeper contact angles would be expected to result in a greater force being transmitted axially along the length of the microtubule and thereby increase the probability of microtubule catastrophe. Besides the involvement of mechanical forces, steep-angle collisions may also promote microtubule catastrophe by affecting the activity and/or binding accessibility of MAPs such as MAP65 and plus-end binding proteins.

Besides facilitating the maintenance of the transverse array, microtubule zippering and catastrophic collisions represent rules of microtubule behavior that are important for the formation of ordered cortical microtubule arrays. Specifically, Monte Carlo modeling showed that these rules can result in the emergence of a parallel microtubule arrangement from a randomly arranged population of simulated microtubules. The model also revealed that both microtubule zippering and catastrophic collisions are required for the generation of microtubule order (i.e., these two processes act synergistically to generate microtubule order). However, we note that future modeling using much larger numbers of microtubules and iterations may reveal subtleties regarding the relative importance of these rules under different situations. Our Monte Carlo modeling resulted in fewer microtubules at the end because we did not incorporate microtubule nucleation in the modeling process. Incorporation of microtubule nucleation would predictably prevent a net loss of microtubules but nonetheless give rise to the same qualitative outcome (i.e., regional microtubule parallel organization).

Importantly, control simulations that did not impose these rules on the dynamics of the simulated microtubules did not generate microtubule bundling or parallel organization, indicating that the modification of the stochastic cortical microtubule dynamics by microtubule interactions is essential for microtubule organization into parallel arrays. The importance of microtubule interactions for their parallel organization was further emphasized by the observation that short microtubules, which do not encounter one another, remain randomly arranged. This result is strikingly similar to the cortical microtubule phenotype of the *mor1* mutant at the restrictive temperature (Whittington et al., 2001) and suggests the possibility that cortical microtubule disorganization at the restrictive temperature is the outcome of shortened cortical microtubules.

Based on these results, we propose that microtubule zippering and catastrophic collisions represent two simple rules that define the outcome of proximate microtubule interactions and lead to parallel microtubule organization. It is important to note that although these rules are sufficient to model the emergence of microtubule parallel organization, they alone cannot account for the establishment of the transverse orientation of cortical arrays in elongating cells. Therefore, additional factors (e.g., seeding through the selective stabilization of microtubules in the transverse orientation) must be involved to direct the organization of cortical microtubules in the transverse orientation.

The results from the Monte Carlo modeling are consistent with several known properties of the cortical microtubule array. (1) The results of the model show that the emergence of parallel microtubule organization does not require that microtubules have the same plus-end orientation. This outcome is consistent with the mixed plus-end orientation of the cortical microtubule array (Dhonukshe and Gadella, 2003; Shaw et al., 2003; Tian et al., 2004; Vos et al., 2004). (2) The results of the model are consistent with the observation that cortical array organization does not require complete depolymerization of the microtubules followed by polymerization in a specific orientation (Wasteney and Williamson, 1989; Wymer et al., 1996). (3) The results of the model are consistent with the observation that cortical microtubule array organization occurs progressively starting with a random orientation of microtubules, followed by the emergence of local parallel organization, which ultimately resolves into a net global parallel organization (Hepler et al., 1993; Wasteney et al., 1993; Yuan et al., 1994; Wymer et al., 1996).

METHODS

Cell Cultures

The *Nicotiana tabacum* cv BY-2 cell cultures were maintained at 26°C on a rotary platform shaker at 100 rpm. The cells were subcultured weekly using a ratio of 1:50 of cell culture to liquid medium (3% sucrose, 4.3 g/L Murashige and Skoog basal salts, 100 mg/L myo-inositol, 1 mg/L thiamine, 0.2 mg/L 2,4-D, and 255 mg/L KH₂PO₄, pH 5.7). Cells were used for microscopy 2 to 3 d after subculture.

Microscopy

All observations were performed on living cells, immobilized on poly-L-Lys-coated cover slips, in a humid chamber. Images were collected using either a Plan-Neofluar 40× (1.3 numerical aperture) or 100× (1.3 numerical aperture) oil-immersion objective (Zeiss, Thornwood, NY).

Wide-field microscopy was conducted with a shutter-equipped Zeiss Axiovert S100 TV microscope on a vibration-isolation table. Images were captured with a CoolSNAP HQ camera (Roper Scientific, Tucson, AZ) using 5 to 10% excitation light intensity from a 100-W mercury arc-lamp. Pixels were not binned to preserve maximal spatial resolution of microtubule ends. DsRed (530 to 560 nm excitation, 570 to 650 nm emission) and YFP (490 to 510 nm excitation, 520 to 550 nm emission) filter sets were used to visualize the fluorophores.

Cortical microtubule dynamics in MBD-DsRed-expressing cells were typically visualized by capturing images with a 1-s camera exposure time, at 5-s intervals, for ~10 min. The time-lapse interval was increased to 10 to 15 s for observations of YFP-TUA6-expressing cells to prevent photobleaching of YFP.

Quantification of the Cortical Microtubule Dynamics

Only those microtubules that remained in the focal plane during the observation period, and therefore presumably plasma membrane bound, were included in the analyses. The dynamic behavior of individual microtubule plus-ends was tracked frame-by-frame, from time-lapse sequences, and the relative change in microtubule length with respect to the starting position was determined using the measure length feature of ESee (Inovision, Durham, NC). This information was imported into Excel (Microsoft, Seattle, WA) to generate life history plots, which were used to determine the dynamic instability parameters.

Only changes in microtubule length $>0.25 \mu\text{m}/\text{frame}$ were considered growth or shrinkage events. The growth and shrinkage rates were determined for the appropriate phases using regression analysis. The rescue frequency was calculated by dividing the sum of the number of transitions from shrinkage to growth, and from shrinkage to pause, by the time spent shrinking. The catastrophe frequency was calculated by dividing the sum of the number of transitions from growth to shrinkage, and from pause to shrinkage, by the sum of the time spent growing and pausing. The dynamicity was calculated as the sum of the total lengths grown and shortened per minute. The relative time spent growing, shrinking, and pausing was calculated from the sum of the durations that a microtubule population spent growing, shrinking, and pausing.

An encounter between cortical microtubules was defined as an event when a growing microtubule appeared to come in contact with a pre-existing microtubule. The angle of contact during such encounters was determined manually, and the time period between the first frame of microtubule contact to the first frame of loss of microtubule contact was used as the microtubule contact time.

Statistical analyses were conducted using the Analyze-It add-in (Analyze-It Software, Leeds, UK) for Excel. Data sets were first tested to determine whether they conformed to a normal distribution using the Shapiro-Wilk *W*-test. The Student's *t* test was used for the analysis of normally distributed data sets, and the Mann-Whitney nonparametric test was used for the analysis of non-normally distributed data sets.

Monte Carlo Modeling of the Dynamic Microtubule Behavior

The Monte Carlo modeling was conducted using a combination of Excel and Corel Draw (Corel, Dallas, TX). The random number generator function in Excel was used to randomly assign the starting position, angle, and orientation of the plus-ends of 20 simulated microtubules in a 4×5 grid. In most cases, the simulated microtubules were 4 cm in length. In the case of the simulation with short microtubules (Figure 7), the microtubules were 2 cm in length. Each microtubule was centered within the square it occupied in the grid. The simulated microtubules that were oriented at an angle of 0 to 45° relative to the long axis of the grid were considered longitudinal, whereas those oriented at an angle of 46 to 90° relative to the long axis of the grid were considered transverse.

The dynamic behavior of the simulated microtubules was modeled iteratively using the parameters shown in Tables 1 and 2, with the iterations representing 1 min. Specifically, the random number function was used to determine which of the transverse and longitudinal microtubules would grow, shrink, or pause at the rates shown in Table 1.

Apparent microtubule interactions in the starting frame were not included in the simulation, and we defined a microtubule encounter as an event in which a growing microtubule end contacts another microtubule. Therefore, microtubule encounters did not occur until after the first iteration. The consequence of these microtubule encounters was contingent on the angle at which the encounters occurred and whether the microtubule in question was longitudinal or transverse. Microtubules experiencing shallow-angle encounters were constrained from shrinking (i.e., they either grew or paused) for one (for longitudinal) or two (for transverse) iterations 90% of the time (based on the percentage of shallow-angle encounters that led to zippering), and the direction of their growing ends was changed to align them with the encountered microtubule. On the other hand, microtubules experiencing steep-angle encounters were forced to shrink in the next iteration 60% of the time (based on the percentage of steep-angle encounters that led to catastrophes). Microtubules that encountered the edge of the simulation space were allowed to behave stochastically (i.e., there were no edge effects).

Control simulations, which did not implement microtubule zippering or catastrophic collisions, used the same initial microtubule configurations

and the dynamics for the first iteration as the corresponding experimental run. Subsequent iterations were conducted based on the randomly assigned behavior for each microtubule.

ACKNOWLEDGMENTS

We thank Andy Miller for generating the YFP-TUA6 tobacco cell line and Deb Fisher for critical reading of the manuscript. This work was supported by USDA Grant 98-35304-6668 and Department of Energy Grant DE-FG02-91ER20050.

Received August 16, 2004; accepted September 20, 2004.

REFERENCES

- Azimzadeh, J., Traas, J., and Pastuglia, M. (2001). Molecular aspects of microtubule dynamics in plants. *Curr. Opin. Plant Biol.* **4**, 513–519.
- Baskin, T.I. (2001). On the alignment of cellulose microfibrils by cortical microtubules: A review and a model. *Protoplasma* **215**, 150–171.
- Baskin, T.I., Beemster, G.T.S., Judy-March, J.E., and Marga, F. (2004). Disorganization of cortical microtubules stimulates tangential expansion and reduces the uniformity of cellulose microfibril alignment among cells in the root of *Arabidopsis*. *Plant Physiol.* **135**, 1–12.
- Burk, D.H., and Ye, Z.H. (2002). Alteration of oriented deposition of cellulose microfibrils by mutation of a katanin-like microtubule-severing protein. *Plant Cell* **14**, 2145–2160.
- Chan, J., Calder, G.M., Doonan, J.H., and Lloyd, C.W. (2003). EB1 reveals mobile microtubule nucleation sites in *Arabidopsis*. *Nat. Cell Biol.* **5**, 967–971.
- Chan, J., Jensen, C.G., Jensen, L.C.W., Bush, M., and Lloyd, C.W. (1999). The 65-kDa carrot microtubule-associated protein forms regularly arranged filamentous cross-bridges between microtubules. *Proc. Natl. Acad. Sci. USA* **96**, 14931–14936.
- Cyr, R.J. (1994). Microtubules in plant morphogenesis: Role of the cortical array. *Annu. Rev. Cell Biol.* **10**, 153–180.
- Cyr, R.J., and Palevitz, B.A. (1989). Microtubule-binding proteins from carrot. 1. Initial characterization and microtubule bundling. *Planta* **177**, 245–260.
- Cytrynbaum, E.N., Rodionov, V., and Mogilner, A. (2004). Computational model of dynein-dependent self-organization of microtubule asters. *J. Cell Sci.* **117**, 1381–1397.
- Dhonukshe, P., and Gadella, T.W., Jr. (2003). Alteration of microtubule dynamic instability during preprophase band formation revealed by yellow fluorescent protein-CLIP170 microtubule plus-end labeling. *Plant Cell* **15**, 597–611.
- Dhonukshe, P., Laxalt, A.M., Goedhart, J., Gadella, T.W.J., and Munnik, T. (2003). Phospholipase D activation correlates with microtubule reorganization in living plant cells. *Plant Cell* **15**, 2666–2679.
- Dixit, R., and Cyr, R. (2003). Cell damage and reactive oxygen species production induced by fluorescence microscopy: Effect on mitosis and guidelines for non-invasive fluorescence microscopy. *Plant J.* **36**, 280–290.
- Dogterom, M., and Yurke, B. (1997). Measurement of the force-velocity relation for growing microtubules. *Science* **278**, 856–860.
- Gardiner, J., Collings, D.A., Harper, J.D.I., and Marc, J. (2003). The effects of the phospholipase D-antagonist 1-butanol on seedling development and microtubule organization in *Arabidopsis*. *Plant Cell Physiol.* **44**, 687–696.
- Gardiner, J., and Marc, J. (2003). Putative microtubule-associated proteins from the *Arabidopsis* genome. *Protoplasma* **222**, 61–74.

- Gardiner, J.C., Harper, J.D.I., Weerakoon, N.D., Collings, D.A., Ritchie, S., Gilroy, S., Cyr, R.J., and Marc, J.** (2001). A 90-kD phospholipase D from tobacco binds to microtubules and the plasma membrane. *Plant Cell* **13**, 2143–2158.
- Goddard, R.H., Wick, S.W., Silflow, C.D., and Snustad, D.P.** (1994). Microtubule components of the plant cell cytoskeleton. *Plant Physiol.* **104**, 1–6.
- Granger, C.L., and Cyr, R.J.** (2001). Spatiotemporal relationships between growth and microtubule orientation as revealed in living root cells of *Arabidopsis thaliana* transformed with green-fluorescent-protein gene construct GFP-MBD. *Protoplasma* **216**, 201–214.
- Hardham, A.R., and Gunning, B.E.S.** (1978). Structure of cortical microtubule arrays in plant cells. *J. Cell Biol.* **77**, 14–34.
- Hashimoto, T.** (2003). Dynamics and regulation of plant interphase microtubules: A comparative view. *Curr. Opin. Plant Biol.* **6**, 568–576.
- Hepler, P.K., Cleary, A.L., Gunning, B.E.S., Wadsworth, P., Wasteneys, G.O., and Zhang, D.H.** (1993). Cytoskeletal dynamics in living plant cells. *Cell Biol. Int.* **172**, 127–142.
- Hussey, P.J., Hawkins, T.J., Igarashi, H., Kaloriti, D., and Smertenko, A.** (2002). The plant cytoskeleton: Recent advances in the study of the plant microtubule-associated proteins MAP-65, MAP-190 and the *Xenopus* MAP215-like protein, MOR1. *Plant Mol. Biol.* **50**, 915–924.
- Janson, M.E., de Dood, M.E., and Dogterom, M.** (2003). Dynamic instability of microtubules is regulated by force. *J. Cell Biol.* **161**, 1029–1034.
- Jiang, C.J., and Sonobe, S.** (1993). Identification and preliminary characterization of a 65-kDa higher-plant microtubule-associated protein. *J. Cell Sci.* **105**, 891–901.
- Lloyd, C.** (1994). Why should stationary plants cells have such dynamic microtubules? *Mol. Biol. Cell* **5**, 1277–1280.
- Lloyd, C., and Chan, J.** (2004). Microtubules and the shape of plants to come. *Nat. Rev. Mol. Cell Biol.* **5**, 13–22.
- Lloyd, C., Drobak, B., Dove, S., and Staiger, C.** (1996). Interactions between the plasma membrane and the cytoskeleton in plants. In *Membranes: Specialized Functions in Plants*, M. Smallwood, J. Knox, and D. Bowles, eds (Herndon, VA: Bios), pp. 1–20.
- Maly, I.V., and Borisy, G.G.** (2002). Self-organization of treadmilling microtubules into a polar array. *Trends Cell Biol.* **12**, 462–465.
- Marc, J., Granger, C.L., Brincat, J., Fisher, D.D., Kao, Th., McCubbin, A.G., and Cyr, R.J.** (1998). A GFP-MAP4 reporter gene for visualizing cortical microtubule rearrangements in living epidermal cells. *Plant Cell* **10**, 1927–1940.
- Mathur, J., Mathur, N., Kernebeck, B., Srinivas, B.P., and Hulskamp, M.** (2003). A novel localization pattern for an EB1-like protein links microtubule dynamics to endomembrane organization. *Curr. Biol.* **13**, 1991–1997.
- McNiven, M.A., and Porter, K.R.** (1988). Organization of microtubules in centrosome-free cytoplasm. *J. Cell Biol.* **106**, 1593–1605.
- Nedelec, F.** (2002). Computer simulations reveal motor properties generating stable antiparallel microtubule interactions. *J. Cell Biol.* **158**, 1005–1015.
- Reddy, A.S.** (2001). Molecular motors and their functions in plants. *Int. Rev. Cytol.* **204**, 97–178.
- Schellenbaum, P., Vantard, M., and Lambert, A.M.** (1992). Higher plant microtubule-associated proteins (MAPs): A survey. *Biol. Cell.* **76**, 359–364.
- Shaw, S.L., Kamyar, R., and Ehrhardt, D.W.** (2003). Sustained microtubule treadmilling in *Arabidopsis* cortical arrays. *Science* **300**, 1715–1718.
- Smertenko, A., Saleh, N., Igarashi, H., Mori, H., Hauser-Hahn, I., Jiang, C.J., Sonobe, S., Lloyd, C.W., and Hussey, P.J.** (2000). A new class of microtubule-associated proteins in plants. *Nat. Cell Biol.* **2**, 750–753.
- Smith, L.G.** (2003). Cytoskeletal control of plant cell shape: Getting the fine points. *Curr. Opin. Plant Biol.* **6**, 63–73.
- Sonobe, S., Yamamoto, S., Motomura, M., and Shimmen, T.** (2001). Isolation of cortical MTs from tobacco BY-2 cells. *Plant Cell Physiol.* **42**, 162–169.
- Sugimoto, K., Himmelspach, R., Williamson, R.E., and Wasteneys, G.O.** (2003). Mutation or drug-dependent microtubule disruption causes radial swelling without altering parallel cellulose microfibril deposition in *Arabidopsis* root cells. *Plant Cell* **15**, 1414–1429.
- Sugimoto, K., Williamson, R.E., and Wasteneys, G.O.** (2000). New techniques enable comparative analysis of microtubule orientation, wall texture, and growth rate in intact roots of *Arabidopsis*. *Plant Physiol.* **124**, 1493–1506.
- Tian, G.-W., Smith, D., Glück, S., and Baskin, T.I.** (2004). Higher plant cortical microtubule array analyzed in vitro in the presence of the cell wall. *Cell Motil. Cytoskeleton* **57**, 26–36.
- Ueda, K., Matsuyama, T., and Hashimoto, T.** (1999). Visualization of microtubules in living cells of transgenic *Arabidopsis thaliana*. *Protoplasma* **206**, 201–206.
- Vesk, P.A., Vesk, M., and Gunning, B.E.S.** (1996). Field emission scanning electron microscopy of microtubule arrays in higher plant cells. *Protoplasma* **195**, 168–182.
- Vorobjev, I., Malikov, V., and Rodionov, V.** (2001). Self-organization of a radial microtubule array by dynein-dependent nucleation of microtubules. *Proc. Natl. Acad. Sci. USA* **98**, 10160–10165.
- Vos, J.W., Dogterom, M., and Emons, A.M.** (2004). Microtubules become more dynamic but not shorter during preprophase band formation: A possible “search-and-capture” mechanism for microtubule translocation. *Cell Motil. Cytoskeleton* **57**, 246–258.
- Wasteneys, G.O.** (2002). Microtubule organization in the green kingdom: Chaos or self-order? *J. Cell Sci.* **115**, 1345–1354.
- Wasteneys, G.O., and Galway, M.E.** (2003). Remodeling the cytoskeleton for growth and form: An overview with some new views. *Annu. Rev. Plant Biol.* **54**, 691–722.
- Wasteneys, G.O., Gunning, B.E.S., and Hepler, P.K.** (1993). Microinjection of fluorescent brain tubulin reveals dynamic properties of cortical microtubules in living plant cells. *Cell Motil. Cytoskeleton* **24**, 205–213.
- Wasteneys, G.O., and Williamson, R.E.** (1989). Reassembly of microtubules in *Nitella tasmanica*: Quantitative analysis of assembly and orientation. *Eur. J. Cell Biol.* **50**, 76–83.
- Whittington, A.T., Vugrek, O., Wei, K.J., Hasenbein, N.G., Sugimoto, K., Rashbrooke, M.C., and Wasteneys, G.O.** (2001). MOR1 is essential for organizing cortical microtubules in plants. *Nature* **411**, 610–613.
- Wicker-Planquart, C., Stoppin-Mellet, V., Blanchoin, L., and Vantard, M.** (2004). Interactions of tobacco microtubule-associated protein MAP65-1b with microtubules. *Plant J.* **39**, 126–134.
- Williamson, R.E.** (1991). Orientation of cortical microtubules in interphase plant cells. *Int. Rev. Cytol.* **129**, 135–206.
- Wymer, C.L., Fisher, D.D., Moore, R.C., and Cyr, R.J.** (1996). Elucidating the mechanism of cortical microtubule reorientation in plant cells. *Cell Motil. Cytoskeleton* **35**, 162–173.
- Yuan, M., Shaw, P.J., Warn, R.M., and Lloyd, C.W.** (1994). Dynamic reorientation of cortical microtubules, from transverse to longitudinal, in living plant cells. *Proc. Natl. Acad. Sci. USA* **91**, 6050–6053.

Encounters between Dynamic Cortical Microtubules Promote Ordering of the Cortical Array through Angle-Dependent Modifications of Microtubule Behavior

Ram Dixit and Richard Cyr

Plant Cell 2004;16;3274-3284; originally published online November 11, 2004;

DOI 10.1105/tpc.104.026930

This information is current as of December 1, 2020

Supplemental Data	/content/suppl/2004/11/04/tpc.104.026930.DC1.html
References	This article cites 53 articles, 21 of which can be accessed free at: /content/16/12/3274.full.html#ref-list-1
Permissions	https://www.copyright.com/ccc/openurl.do?sid=pd_hw1532298X&issn=1532298X&WT.mc_id=pd_hw1532298X
eTOCs	Sign up for eTOCs at: http://www.plantcell.org/cgi/alerts/ctmain
CiteTrack Alerts	Sign up for CiteTrack Alerts at: http://www.plantcell.org/cgi/alerts/ctmain
Subscription Information	Subscription Information for <i>The Plant Cell</i> and <i>Plant Physiology</i> is available at: http://www.aspb.org/publications/subscriptions.cfm